International Journal for Parasitology 49 (2019) 355–364

Contents lists available at ScienceDirect

International Journal for Parasitology

journal homepage: www.elsevier.com/locate/ijpara

14-3-3 protein and ubiquitin C acting as SjIAP interaction partners facilitate tegumental integrity in *Schistosoma japonicum*

Juntao Liu, Bikash Ranjan Giri, Yongjun Chen, Guofeng Cheng *

Shanghai Veterinary Research Institute, Chinese Academy of Agricultural Sciences, Key Laboratory of Animal Parasitology of Ministry of Agriculture, 200241, China

ARTICLE INFO

Article history:
Received 27 July 2018
Received in revised form 16 November 2018
Accepted 20 November 2018
Available online 22 February 2019

Keywords:
Schistosoma japonicum
Apoptosis
14-3-3 protein
Ubiquitin C
Tegument integrity

ABSTRACT

Schistosomiasis, caused by trematodes of the genus *Schistosoma*, remains an important public health issue. Adult schistosomes can survive in the definitive host for several decades, although they are subject to the host immune response. Consequently, understanding the mechanism underlying worm survival in the definitive hosts could aid in developing novel strategies against schistosomiasis. We previously found that an inhibitor of apoptosis in *Schistosoma japonicum* (SjIAP) could negatively regulate apoptosis by inhibiting caspase activity, which plays a critical role in maintaining tegument integrity. The current study aimed to further analyze the mechanism related to SjIAP governing worm tegument integrity; therefore, we used a yeast two-hybrid screen and identified a series of putative interacting partners of SjIAP, including 14-3-3 (Sj14-3-3) and ubiquitin C (SjUBC). Quantitative real time PCR (qRT-PCR) analysis indicated that transcript profiles of *Sj14-3-3* and *SjUBC* increased together with worm development in definitive hosts, which corresponds to those of *SjIAP* in *S. japonicum*. Immunohistochemical analysis showed Sj14-3-3 and SjUBC were located in the tegument of adult parasites while they were also ubiquitously distributed in the bodies of worms. Silencing of *Sj14-3-3*/*SjUBC* expression led to increased caspase activity and induced worm death. Inhibition of Sj14-3-3 or SjUBC resulted in significant morphological alterations in the schistosome tegument. Overall, our findings indicated that Sj14-3-3 and SjUBC interacting with SjIAP may belong to another strategy of *S. japonicum* to maintain the tegument integrity.

1. Introduction

Schistosomiasis is a zoonotic disease that affects more than 200 million people in 76 tropical and subtropical countries (Hotez et al., 2014). Further, it contributes to approximately 300,000 deaths annually in developing countries of Africa, the Middle East, and southeastern Asia (Colley et al., 2014). Adult schistosomes can survive for decades inside the definitive host and lay hundreds to thousands of eggs per day, which is the main cause of its pathology (Cheng et al., 2005). However, there is no effective vaccine against schistosomiasis and current treatment is highly dependent on praziquantel chemotherapy (Thetiot-Laurent et al., 2013). Unfortunately, large doses and frequent administration of the drug may lead to drug resistance (Vale et al., 2017). Consequently, understanding the mechanism underlying schistosome survival in definitive hosts may help to develop novel strategies to control schistosomiasis.

Apoptosis is a form of programmed cell death that is essential for tissue homeostasis during the development of metazoans (Kerr et al., 1972; Williams, 1994; Peng et al., 2011). Recent studies have indicated that parasites not only manipulate host apoptotic pathways to support their survival in the final hosts but also negatively regulate apoptotic processes to modulate cellular functions in response to a hostile environment and in the presence of an immune response. For example, Lee and coworkers demonstrated that a Bcl-2 family apoptotic inhibitor can negatively regulate apoptotic processes in *Schistosoma mansoni* (Lee et al., 2011, Lee et al., 2014). In addition, inhibitor of apoptosis proteins (IAPs) represent a highly conserved protein family that supports pro-survival signaling pathways by preventing the effector phase of apoptosis (Scott et al., 2005; Silke and Meier, 2013). Moreover, IAPs are also involved in the regulation of other processes such as cell division, morphogenesis, heavy metal homeostasis, NF-kB activation, the immune response, and mitogen-activated protein kinase signal transduction pathways (Srinivasula and Ashwell, 2008; Silke and Meier, 2013).

* Corresponding author at: Shanghai Veterinary Research Institute, Chinese Academy of Agricultural Sciences, Key Laboratory of Animal Parasitology of Ministry of Agriculture, 518 Ziyue Road, Shanghai 200241, China. Fax: +86 215 408 1818.
E-mail address: chengguofeng@caas.cn (G. Cheng).

https://doi.org/10.1016/j.ijpara.2018.11.011
0020-7519/

In our previous study, we found that expression of the *Schistosoma japonicum* IAP gene (*SjIAP*) was increased in the definitive host (Peng et al., 2010), suggesting that it might be involved in parasitism. Further evaluation of recombinant SjIAP suggested that it provides moderate protection against schistosome infection and that it is a potential vaccine candidate for schistosomiasis (Hu et al., 2014). Our recent studies also indicated that SjIAP plays an important role in maintaining tegument integrity by negatively regulating cellular apoptosis (Liu et al., 2018). Here, we further analyzed the mechanisms underlying the involvement of the SjIAP in regulating apoptosis and tegument integrity by utilizing a yeast two hybridization (Y2H) system to identify putative interacting partners of SjIAP, and evaluating the roles of the selected partners in caspase inhibition and the maintenance of tegument integrity using small interfering RNAs (siRNAs).

2. Materials and methods

2.1. Ethics statement

All animal experiments were carried out in strict accordance with the recommendations in the Guide for the Care and Use of Laboratory Animals of the Ministry of Science and Technology of the People's Republic of China. All efforts were made to minimize suffering. All animal procedures were approved by the Animal Management Committee and the Animal Care and Use Committee of Shanghai Science and Technology Commission of Shanghai municipal government for the Shanghai Veterinary Research Institute, Chinese Academy of Agricultural Sciences, China (Permit number: SYXK 2016–0010).

2.2. Schistosoma japonicum maintenance and parasite collection

The life cycle of *S. japonicum* (Anhui isolate) was maintained in New Zealand rabbits and BALB/c mice together with *Oncomelania hupensis* (Center of National Institute of Parasitic Disease, Chinese Center for Disease Control and Prevention, Shanghai, China) as the snail host. Unless indicated otherwise, New Zealand rabbits and BALB/c mice were infected with approximately 1,000 and 100 cercariae, respectively, by inoculating the shaved abdominal skin surface with a moist cercarial paste. To collect schistosomes at different developmental stages, the parasites were perfused from the rabbits at 14, 21, 28 and 35 days of post infection. The eggs were isolated from the livers of infected animals following a standard protocol described previously (Lewis et al., 1986). The eggs and parasites were snap-frozen in liquid nitrogen until use.

2.3. Construction of a Y2H library for adult S. japonicum

Total RNA was isolated from adult schistosomes as described elsewhere (Peng et al., 2010; Cheng et al., 2013). Poly(A+)-RNA purification was carried out using the Oligotex mRNA mini kit (Qiagen, Germany) as per the manufacturer's instructions. The DUAL membrane starter kit (Dualsystems Biotech, Switzerland) was used to generate a Y2H library for adult *S. japonicum* (Y2HSJ). Briefly, first-strand cDNA was synthesized using 1.2 μg of poly(A+) mRNA from adult worms with oligo(dT)-priming. After the tailing reaction and amplification of double-stranded (ds) DNA by long-distance PCR, fragments less than 1000 bp were discarded by gel purification. The remaining cDNAs were cloned via a recombination step into a pPR3-N prey vector (Dualsystems Biotech, Zürich, Switzerland). Transformants were selected on luria broth (LB) agar with 100 μg/ml of ampicillin and the value of colony forming units for the library was calculated; aliquots were stored at −80 °C.

2.4. Cloning of the bait vectors and evaluation of self-activation

SjIAP was amplified by performing PCR using a recombinant plasmid and the following primers (forward, 5′-AAGGCCAT TACGGCCATGTCTTATTTTCAGAACCTGTCAAAT-3′; reverse, 5′-CCGG CCGAGGCGGCCCCTTTTGGAACATTATTGCTGTGAGTT-3′, with each containing an *Sfi* I restriction site) (Peng et al., 2010). PCR products were cloned via the *Sfi* I site into pBT3SUC vectors (Dualsystems Biotech). The recombinant pBT3SUC-SjIAP plasmids were further confirmed by sequencing.

To evaluate the potential self-activation of the recombinant pBT3SUC-SjIAP plasmid, the following different combinations were transformed into NMY32 yeast cells: positive control (pNubG-Fe65 + pTSU2-APP), negative control (pPR3N + pTSU2-APP), self-activation evaluation (pPR3N + pBT3SUC-SjIAP), and functional evaluation (pOST1-NubI + pBT3SUC-SjIAP) (Supplementary Table S1). The transformed yeast cells were further cultured at 30 °C for 4 days on different synthetic defined (SD) media (Dualsystems Biotech) including SD-Trp-Leu, SD-Trp-Leu-His, and SD-Trp-Leu-His-Ade, and the number of colonies counted.

2.5. Screening of a Y2HSJ library and sequencing analyses

Y2HSJ screening was performed using the SjIAP as bait against the library as described below. Briefly, plasmids from the Y2HSJ library were transformed into NMY32 yeast cells containing the pBT3SUC-SjIAP bait plasmid and then cultured on SD-Trp-Leu-His + 5 mM 3AT agar. The yeast colonies that grew on the selective agar were inoculated to SD-Trp-Leu agar and analyzed for lacZ reporter expression using a β-galactosidase assay (HTX Kit: Dualsystems Biotech). To identify the cDNA sequence of each colony, each positive colony was inoculated in SD-Trp-Leu liquid media for culture. Then, the plasmids from yeast cells were isolated using the Yeast Plasmid Extraction Kit (Beijing Solarbio Science & Technology Co., Ltd., Beijing, China). The isolated plasmids were further transformed into competent *Escherichia coli* cells for plasmid amplification and subsequently isolated using the Axygen mini plasmid preparation kit (Axygen, NY, USA). The obtained plasmids were then submitted for sequencing using the Sanger DNA sequence method. Sequences were analyzed by BLAST and the domains of putative proteins were analyzed by InterPro (http://www.ebi.ac.uk/interpro/) and SMART (http://smart.embl-heidelberg.de/).

2.6. Confirmation of putative interacting partners by re-transformation of prey plasmid into a yeast-containing bait plasmid

To further confirm interacting partners, NMY32 yeast cells containing the bait plasmid pBT3SUC-SjIAP were prepared as competent cells. Then, 40 prey plasmids were re-transformed into the yeast competent cells to confirm the interaction with SjIAP. Upon transformation, 100 μl of transformation solution were first plated onto SD-Trp-Leu agar. The cultured cells were then further inoculated onto an SD-Trp-Leu plate and SD-Trp-Leu-His-Ade + 10 mM 3AT plate. Positive colonies from the plate (SD-Trp-Leu-His-Ade + 10 mM 3AT) were further assessed for β-galactosidase activity (HTX Kit: Dualsystems Biotech).

2.7. Validation of interacting partners of SjIAP using the ProQuest Two-Hybrid System

The identified interacting partners were validated using the ProQuest Two-Hybrid System (Invitrogen, USA). Briefly, the DNA sequences encoding SjIAP was chemically synthesized and then cloned into the bait plasmid pDEST32 provided by the ProQuest Two-Hybrid System with the Gateway cloning system. In addition,

ubiquitin C (UBC) of *S. japonicum* (*SjUBC*, FN315483.1) and 14-3-3 proteins of *S. japonicum* (*Sj14-3-3*, FN322774.1 and FN315545.1) were cloned into the prey plasmid pDEST22. The recombinant plasmids for each insertion were confirmed by sequencing. The combinations of bait and prey plasmids were transformed into yeast MaV203 cells and then spread onto synthetic complete (SC)-Trp-Leu plates as follows: pDEST22-SjUBC + pDEST32-SjIAP, pDEST22- FN315545.1 + pDEST32-SjIAP, pDEST22-FN322774.1 + pDEST32-SjIAP, pEXP22/RalGDS-wt + pEXP32-Krev1 (strong positive control), pEXP22/RalGDS-ml + pEXP32-Krev1 (weak positive control), pEXP22/RalGDS-m2 + pEXP32-Krev1 (negative control), and pDEST22 + pDEST32 (negative control) (Supplementary Table S1). Three colonies from SC-Trp-Leu plates were randomly selected and further plated on SC-Leu-Trp-Ura, SC-Leu-Trp-His + 3AT, and SC-Leu-Trp + 5FOA plates. The plates were incubated at 30 °C for 4 days.

2.8. RNA isolation and Sj14-3-3/UBC expression analysis

Total RNA was extracted from *S. japonicum* samples using TRIzol reagent (Invitrogen) as described previously (Liu et al., 2018). The isolated RNA was quantified using a Nanodrop ND-1000 spectrophotometer (Nanodrop Technologies, Wilmington, DE, USA). cDNAs were transcribed from total RNA with random primers combined with oligo dT primer using a PrimeScript RT reagent Kit (TaKaRa, China). The levels of mRNA at different stages were analyzed by quantitative PCR (qPCR) by using specific primers (*Sj14-3-3*-FN322774.1, forward primer: 5′- ATCTGTCTCCATCCGA CCTTGT-3′; reverse primer: 5′-CGTTCTTCACTTCCTAACTCCG-3′; *Sj14-3-3*-FN315545.1; forward primer: 5′-AAAAAGGTTGTTGA GATGCC-3′; reverse primer: 5′-ACGATACGCCAAGCCG-3′; *SjUBC*, forward primer: 5′-ATTACTTTGGAAGTTGAGCCAAGTG-3′; reverse primer: 5′-GCAAAGATTAAACGTTGTTGATCGG-3′; and primers for the *S. japonicum* nicotinamide adenine dinucleotide (*NADH*) dehydrogenase gene (forward primer: 5′-CGAGGACCTAACAGCA GAGG-3′; reverse primer: 5′-TCCGAACGAACTTTGAATCC-3′) were used as an internal control for normalization. Upon the assessment of efficiencies and specificities of the primers, qPCR was performed using SYBR Premix Ex Taq (TaKaRa). A 20 μl reaction mixture contained 1 μl of cDNA, 10 μl of 2 × SYBR Primer Ex TagII (TaKaRa), 8 μl of H_2O, and 1 μl of primers (10 μM). The reactions were amplified in a Master cycler ep realplex (Eppendorf, Germany) real-time PCR detection system, using the following thermal cycling profile: 95 °C for 5 min, followed by 40 cycles of amplification (94 °C for 5 s, 60 °C for 30 s, 72 °C for 20 s). Relative mRNA expression was calculated using the $2^{-\Delta Ct}$ method (Livak and Schmittgen, 2001).

2.9. Schistosome culture and electroporation

Adult schistosomes (22–25 days old) were cultured in a 12-well plate with 2 mL of complete RPMI-1640 medium containing 2 g/L of glucose, 0.3 g/L of L-glutamine, 2.0 g/L of $NaHCO_3$, 15% FBS (Gibco, USA), and 5% penicillin/streptomycin (10,000 U penicillin and 10 mg of streptomycin in 0.9% NaCl, Gibco) in an incubator with 5% CO_2 at 37 °C. *SjIAP* (siRNA-951: sense CCGCCUACAAAGU CAAUCUTT, antisense AGAUUGACUUUGUAGGCGGTT) *Sj14-3-3* (siRNA-165: sense GGAGUUAGGAAGUGAAGAATT, antisense UUCUUCACUUCCUAACUCCTT; siRNA-321: sense GGAAGAGGAGU UAAACGAATT, antisense UUCGUUUAACUCCUCUUCCTT; siRNA-575: sense CCCUUAACUUCUCAGUGUUTT, antisense AACACUGAGA AGUUAAGGGTT), and *SjUBC* siRNA (siRNA-131: sense CCGAUCAA CAACGUUUAAUTT, antisense AUUAAACGUUGUUGAUCGGTT; siRNA-934: sense CCAGGAAUAAGGAGGAAUUTT, antisense AAUU CCUCCUUAUUCCUGGTT) and control siRNA (Sense UGGCGAAUG GCCGGACACUCCTT, Antisense GGAGUGUCCGGCCAU UCGCAATT) were designed and chemically synthesized by Shanghai GenePharma (China) based on the corresponding sequences obtained from *S. japonicum* of the Chinese mainland strain (Hu et al., 2003). Each siRNA duplex (3 μg per experiment) was delivered into the cultured schistosomes by electroporation at 125 V, 20 ms, one pulse in 200 μL of RPMI 1640 medium. Schistosomes were then transferred to 12-well cell culture plates containing 2 mL of fresh medium. The parasites were usually collected at 4 days post-electroporation for quantitative real time PCR (qRT-PCR) analysis, western blotting, caspase activity assays, and electron microscopy as described subsequently unless otherwise indicated.

2.10. qRT-PCR analysis to determine transcript levels of SjIAP in siRNA-treated worms

Total RNA was isolated from treated and control parasites using TRIzol reagent (Invitrogen), and the isolated RNA was further quantified and cDNA was produced as described previously herein. The mRNA levels of *Sj14-3-3* and *SjUBC* were determined by qRT-PCR using specific primers as described and the *S. japonicum NADH* dehydrogenase gene was used as an internal control. qPCR was performed using SYBR Premix Ex Taq (TaKaRa) as described. Relative mRNA expression was calculated following a method described earlier (Livak and Schmittgen, 2001).

2.11. Western blotting analyses

Protein lysates were prepared from *Sj14-3-3*-, *SjUBC* siRNA, and control siRNA-treated parasites, and were subsequently quantified using a BCA protein assay kit (Beyotime, Shanghai, China). The proteins were subjected to separation via SDS-PAGE (10% resolving gel) and then electrotransferred onto polyvinylidene difluoride membranes (BioRad, USA). Non-specific binding was blocked using non-fat dry milk (5%, Sangon Biotech, China) in PBS (pH 7.4) containing 0.1% Tween 20 (PBST; Sigma-Aldrich, USA). The membranes were incubated for 1 h at room temperature with primary antibodies against 14-3-3 protein (Catalog # 8312S, Cell Signaling Technology, USA), UBC (Catalog # 7780, Abcam, Cambridge, UK) and α-tubulin (Catalog # T6074, Sigma) diluted 1:2000 in blocking buffer. After washing the membrane five times with 0.1% PBST, the membrane was then incubated with horseradish peroxidase-conjugated goat anti-rabbit/mouse IgG secondary antibody (CoWin Biosciences, China) diluted 1:5000 in PBS for 1 h. The membrane was developed using the Immobilon Western Kit according to the manufacturer's instructions (Millipore, Germany). The images were further analyzed using Image J software (https://imagej.nih.gov/ij).

2.12. Immunohistochemistry

Adult schistosomes (28 days old) were fixed in 4% paraformaldehyde overnight at room temperature before being embedded in paraffin. Serial 5 μm thick sections were then cut from the paraffin-embedded blocks, deparaffinized in xylene, and rehydrated through an ethanol series. Endogenous peroxidase activity was quenched with hydrogen peroxidase in methanol (0.3% v/v) for 15 min, followed by three washes with PBS for 1 h, and overnight incubation at 4 °C with primary antibodies against 14-3-3, UBC, SjIAP (positive control) (1:200 dilutions) in PBS containing 3% (w/v) BSA, or PBS containing 3% (w/v) BSA (negative control). Samples were washed three times for 5 min each in 0.02% PBST, and then treated with biotinylated goat anti-rabbit/mice antibody (Abcam) for 20 min at room temperature, which was followed by three additional washes with PBST. Finally, the sections were incubated in streptavidin-horseradish peroxidase for 20 min at room temperature, followed by repeated washes in

PBST. Tissue sections were visualized with 3,3′-diaminobenzidine at room temperature for 5 min, and mounted using Vectashield (Vector Laboratories, Peterborough, UK), and viewed under a microscope equipped with a digital camera.

2.13. Caspase 3/7 activity assay

Parasites were lysed in lysis buffer containing an EDTA-free inhibitor (Roche, Switzerland) as described previously (Cheng et al., 2013). Caspase activity in the protein lysates from siRNA-treated parasites or control parasites was measured using a Glo 3/7 Assay kit (Promega, Madison, WI, USA) and a luminometer (Berthold, Germany). The protein concentration of each protein lysate was used to normalize luciferase activity and was determined using a BCA protein assay kit (Beyotime).

2.14. Viability assessment by Hoechst staining

At 4 days post-electroporation, parasites were collected and then stained with 1 μg/mL of Hoechst 33258 dye for 10 min and examined by fluorescence microscopy (Olympus, Tokyo, Japan) to determine worm viability.

2.15. Electron microscopy analysis

At 4 days post-electroporation, the parasites were collected, washed with PBS (pH 7.4) three times, and then fixed with 4% paraformaldehyde and 2.5% glutaraldehyde (System Biosciences, Mountain View, CA, USA) at 4 °C for 48 h. Samples were post-fixed in osmium tetroxide (1% w/v, System Biosciences) at room temperature and dehydrated with increasing concentrations of acetone (TiTan, Shanghai, China). For scanning electron microscopy (SEM), samples were freeze dried and coated with platinum by sputtering with a plasma multicoater (PMC-500; Mejwafosis, Tokyo, Japan). For transmission electron microscopy (TEM), the dehydrated samples were embedded into resins and cut into thin sections, transferred to metal grids (Agar Scientific, Essex, UK), and stained with uranyl acetate (System Biosciences). Images were captured with a scanning electron microscope (JEOL JSM-6380LV) in a high vacuum mode with an accelerating voltage of 2–10 kV and a transmission electron microscope (JEOL JEM-2010) with an accelerating voltage of 80 kV.

3. Results

3.1. Identification of the putative interacting partners of SjIAP by screening Y2HSJ

To identify the interacting partners of SjIAP, we constructed a Y2HSJ library. Upon the evaluation of self-activation and expression, we used the bait vector pBT3SUC-SjIAP to screen the Y2HSJ. We found that 64 prey clones could grow on the selective plates. After isolation of these prey plasmids, 57/64 clones were successfully sequenced. BLASTX analysis of the sequences of 57 clones indicated that the sequences of eight clones showed no significant homology to the NCBI database, whereas the remaining 49 clones showed high identity to 38 *S. japonicum* genes. Apart from eight genes matching to *S. japonicum* non-coding RNAs or the mitochondrion genome, SMART and InterPro analyses of the domains of other genes indicated that they could be classified into several groups including 14-3-3, ubiquitin homologue, EF-hand, tetratricopeptide repeat-containing domain, major sperm protein domain, acyl-CoA-binding protein, cytochrome c oxidase-like subunit I domain, major facilitator superfamily domain, and beta-catenin-like protein 1 (Table 1). In addition, we noted there were 15 genes showing no significant domains (Table 1).

3.2. Validation of the interacting partners of SjIAP and analysis of Sj14-3-3 and SjUBC transcript levels in parasites with SjIAP inhibition

Previous studies indicated that 14-3-3 is involved in the negative regulation of apoptosis (Clapp et al., 2012) and that IAP can interact with ubiquitin to degrade proteins (Hu and Yang, 2003). In addition, we noted that two 14-3-3 homologues (FN322774.1 and FN315545.1) showed stronger interaction with SjIAP. Therefore, we selected these two Sj14-3-3 homologues and SjUBC for further investigation. Firstly, we independently prepared bait plasmids (pBT3SUC-SjIAP) and the prey plasmids (pPR3N-Sj14-3-3/SjUBC) and then co-transformed them into NMY32 yeast cells. The results indicated the yeast clones survived (Trp2/Leu2/Ade2/His2; Fig. 1A), indicating that SjIAP interacts with Sj14-3-3 in yeast. Next, we used the ProQuest Two-Hybrid System to corroborate these results. As shown in Fig. 1B, co-transformation of SjIAP and Sj14-3-3/SjUBC led to cell survival on selective agar (SC-Leu-Trp-His + 3AT). Cell growth indicated co-transformation with SjIAP and Sj14-3-3/UBC was similar to that for the positive control (weak), suggesting that SjIAP can weakly interact with Sj14-3-3/UBC. In addition, we also determined the transcript levels of *Sj14-3-3* and *SjUBC* in *SjIAP*-inhibited parasites using qRT-PCR. The results indicated that *SjIAP* inhibition led to decreased expression of *Sj14-3-3/SjUBC* (Fig. 1C).

3.3. Expression profiles of Sj14-3-3 and SjUBC at different stages and their localizations

Using qRT-PCR, we determined the expression profiles of *Sj14-3-3* and *SjUBC* at several parasite stages including the egg stage and in parasites collected 14, 21, 28, and 35 days of post infection. *Sj14-3-3* or *SjUBC* expression increased together with worm development in definitive hosts (Fig. 2A). Then, we performed immunohistochemical analysis to determine the localization of Sj14-3-3 and SjUBC using commercial antibodies. Firstly, we validated the

Table 1
Summary of the putative interacting partners of *Schistosoma japonicum* inhibitor of apoptosis protein identified by screening a Y2HSJ library.

Groups	Domains	GenBank IDs (Clone IDs)
1	14-3-3	FN322779.1(30), FN315545.1 (39, 44, 60, 67), FN316174.1(50), FN321076.1(66), FN322774.1(71)
2	Ubiquitin homologue	FN315483.1 (34)
3	EF-hand	FN319199.1(63), FN314828.1(69)
4	Tetratricopeptide repeat-containing domain	FN315443.1 (8), AY812799.1 (52)
5	Major sperm protein domain	FN315407.1 (10)
6	Acyl-CoA-binding protein	FN319231.1 (17, 38)
7	Cytochrome c oxidase-like, subunit I domain	FN314248.1 (47)
8	Major facilitator superfamily domain	FN319761.1 (65)
9	Beta-catenin-like protein 1	AY813413.1 (19)
10	No significant domain	AY814984.1(35), FN323284.1 (22), FN319799.1 (24, 40), FN319737.1(59), FN321260.1(12), AY810132.1(15), FN314164.1(68), FN313877.1(7), FN314281.1(25), AY809338.1(13), FN318301.1(55), FN315866.1(58), AY815222.1 (21), AY811669.1(5), FN315864.1(54),

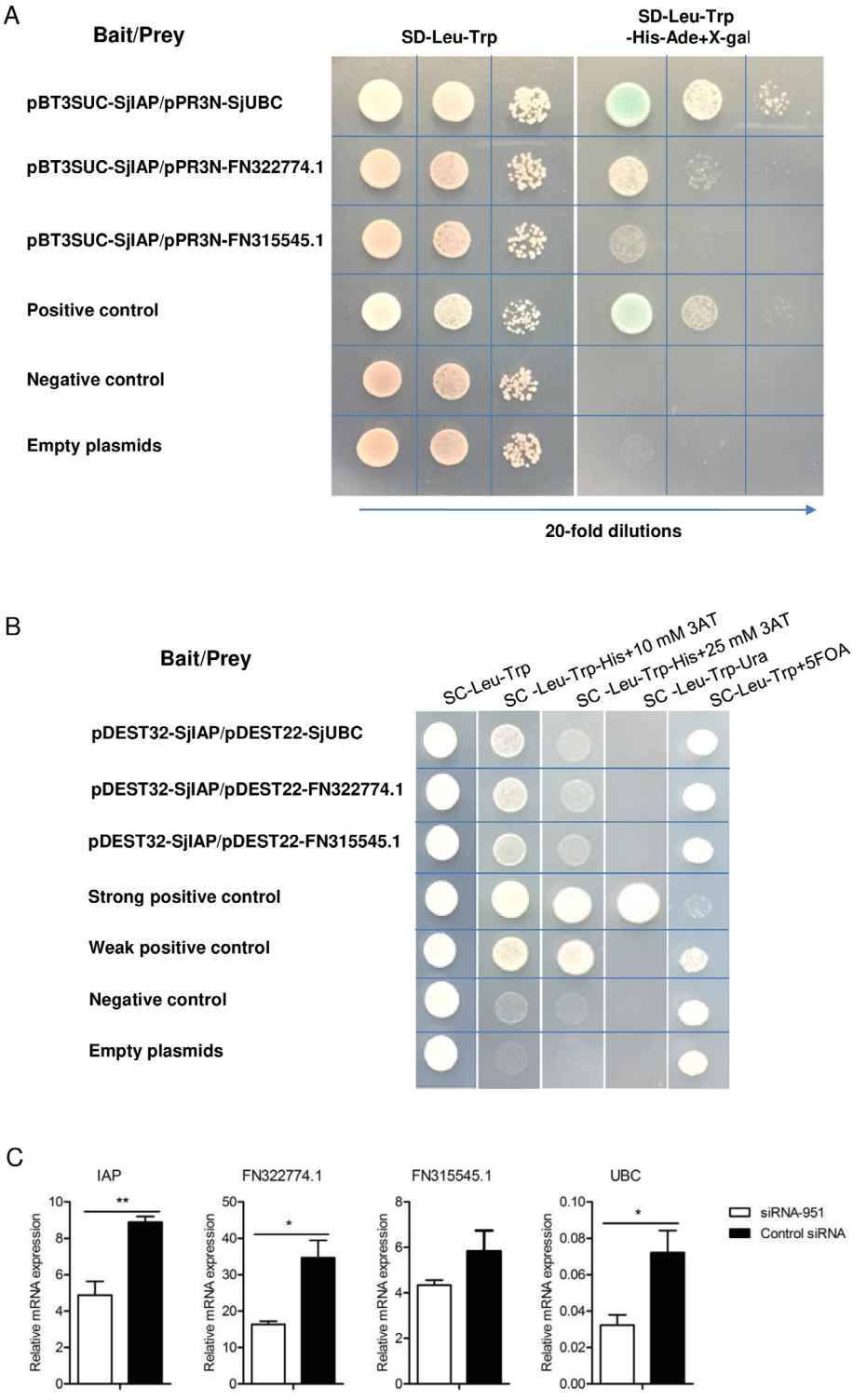

Fig. 1. Validation of *Schistosoma japonicum* inhibitor of apoptosis protein interacting partners and analysis of *S. japonicum* 14-3-3 (*Sj14-3-3*) and *S. japonicum* ubiquitin C (*SjUBC*) gene transcript levels in parasites with inhibitor of apoptosis protein inhibition. (A) Re-transformation of SjIAP- and Sj14-3-3/UBC-encoding plasmids into yeast cells to confirm protein interactions. All diploid yeast strains for which the density was normalized before plating grew equally well under selection for both bait and prey plasmids (SD-Leu-Trp). Twenty-fold dilutions for each diploid sample were plated onto each selection plate. The bait inhibitor of apoptosis protein and prey SjUBC strongly interacted on the reporter plate (SD-Leu-Trp-Ade-His + X-gal). The bait inhibitor of apoptosis protein and prey Sj14-3-3 also interacted, but this appeared to be a weaker interaction compared with that detected for the positive control (pTSU2-APP + pNubG-Fe65) on the reporter plate (Supplementary Table S1). No interaction was detected for the negative control (pPR3N + pTSU2-APP) and empty plasmids (pBT3STE + pPR3N). (B) Validation of the interaction of inhibitor of apoptosis protein and Sj14-3-3/UBC using the ProQuest Two-Hybrid System (Invitrogen, USA)). The bait and prey plasmids were co-transformed into Mav203 yeast cells and three random colonies of yeast cells were spread onto the selection plates; one random colony is shown in B. The bait inhibitor of apoptosis protein and prey proteins (Sj14-3-3/SjUBC) also interacted to support yeast cell survival on SC-Leu-Trp-His + 3AT plates; this appeared to be a weaker interaction than that of the weak positive control (pEXP22/RalGDS-m1 + pEXP32-Krev1) on the reporter plate (Supplementary Table S1). (C) *SjIAP* inhibition led to aberrant levels of *Sj14-3-3/UBC* transcripts. At 4 days post-treatment, total RNA was isolated from the worms, and the mRNA levels of inhibitor of apoptosis protein relative to the reference gene *S. japonicum* nicotinamide adenine dinucleotide dehydrogenase (*SjNADH*) were determined by quantitative real time PCR (qRT-PCR) in parasites transfected with *SjIAP* small interfering RNAs (siRNA) and control siRNA. The data illustrate representative results and show the mean and S.E. derived from triplicate experiments. $^{*}P \leq 0.05$ and $^{**}P \leq 0.01$ (Student's t test, siRNA-951 versus control siRNA).

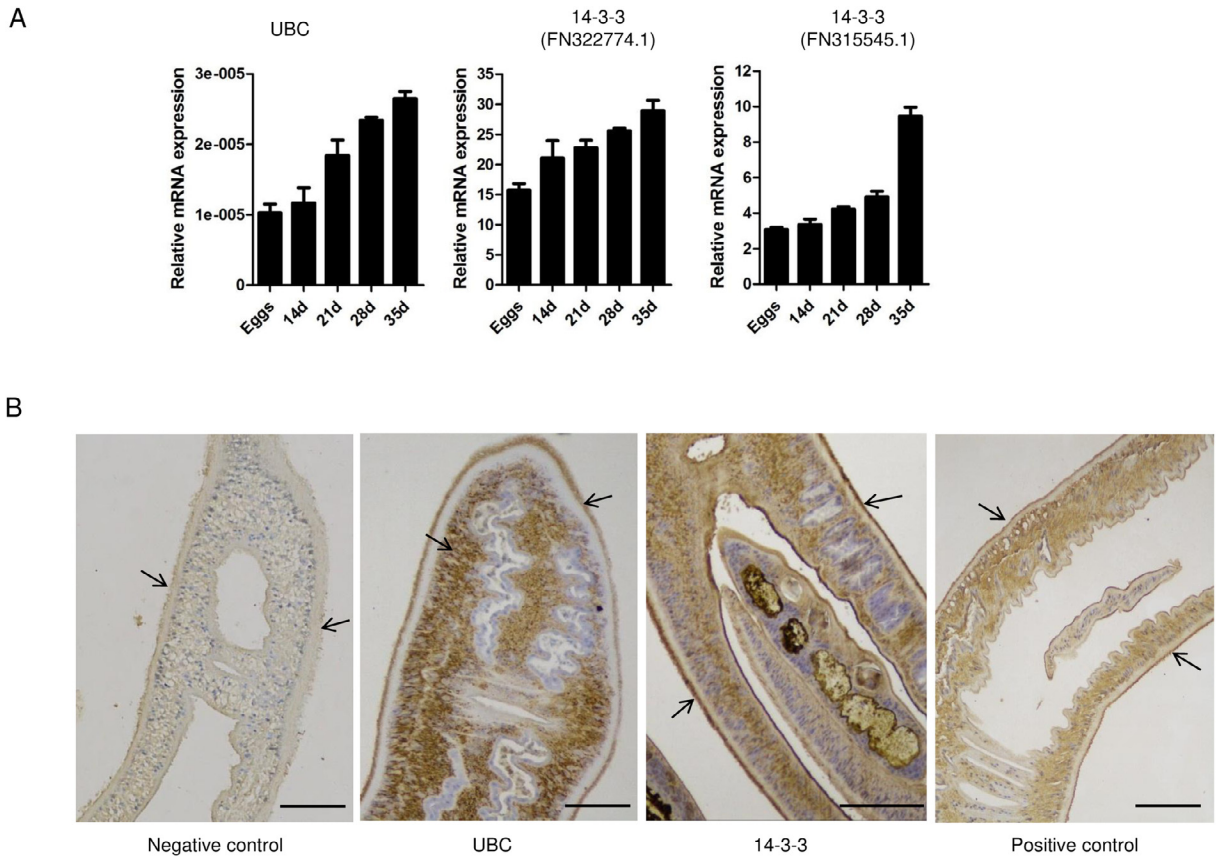

Fig. 2. Expression profiles of *Schistosoma japonicum* 14-3-3 (*Sj14-3-3*) and *S. japonicum* ubiquitin C (*SjUBC*) at different stages and their localizations. (A) Expression of *Sj14-3-3/SjUBC* at different stages in the life cycle of *S. japonicum* from eggs to 35 days (35d). The mRNA expression levels of *Sj14-3-3* and *SjUBC* relative to those of *S. japonicum* nicotinamide adenine dinucleotide dehydrogenase (*SjNADH*) were analyzed by quantitative real time PCR (qRT-PCR). The data illustrate representative results and show the mean and S.E. derived from triplicate experiments. (B) Immunohistochemical analysis of Sj14-3-3 and SjUBC localization in adult schistosomes. A tissue section was incubated with anti-*S. japonicum* inhibitor of apoptosis protein sera as the positive control, and with PBS containing BSA as the negative control. Arrows indicate the schistosome tegument. Bars indicate 50 μm.

specificity of these antibodies by western blotting. The results indicated these antibodies could recognize a single band of *S. japonicum* protein lysates (Supplementary Fig. S1). Immunohistochemical results showed that Sj14-3-3 and SjUBC were located in the tegument of adult parasites while they were also ubiquitously distributed in the body of worms (Fig. 2B).

3.4. Sj14-3-3 silencing results in increased caspase activity and worm mortality

To gain insights into the functions of Sj14-3-3, we designed three siRNA duplexes targeting *Sj14-3-3* mRNA (FN322774.1). Upon electroporation to adult schistosomes, the effects of siRNA silencing on the transcript level of Sj14-3-3 were evaluated by qRT-PCR. The results indicated that each siRNA duplex triggered different effects with respect to silencing *Sj14-3-3*; specifically, siRNA-165 was found to have a marked effect (Fig. 3A). The silencing effect of siRNA-165 was further validated by western blotting (Fig. 3B). Next, we measured caspase 3/7 activity in parasites treated with the siRNA-165 duplex. The results indicated that schistosomes treated with *Sj14-3-3* siRNA had significantly increased caspase 3/7 activity compared with that in parasites treated with control siRNA (Fig. 3C). Furthermore, we delivered this siRNA (siRNA-165) duplex into adult worms and determined its effect on worm mortality. The results showed that siRNA treatment significantly decreased worm survival up to 31% during the 4 day culture period (Fig. 3D).

3.5. SjUBC silencing leads to increased caspase activity and worm death

To determine the functions of SjUBC, we also designed two siRNA duplexes targeting *SjUBC* mRNA and electroporated them into *in vitro* cultured adult schistosomes. The effect of siRNA silencing on the transcript level of *SjUBC* was determined by qRT-PCR. The results indicated that siRNA-131 had a marked effect with respect to *SjUBC* silencing (Fig. 4A). Then, we validated this silencing effect by western blotting (Fig. 4B). The caspase activity in parasites treated with siRNA-131 also significantly increased (Fig. 4C), and this siRNA led to the death of 25% of the worms during in vitro culture (Fig. 4D).

3.6. Silencing of Sj14-3-3 and UBC results in destruction of the tegument in S. japonicum

Given that Sj14-3-3 and SjUBC localized to the tegument of schistosomes and that Sj14-3-3/SjUBC silencing resulted in increased worm death, we used SEM and TEM to investigate morphological alterations in the schistosome tegument following *Sj14-3-3/SjUBC* siRNA treatment. Schistosomes were collected from mice infected with *S. japonicum* cercariae at 22 days of post infection and were then electroporated with *Sj14-3-3/SjUBC* siRNA or control siRNA. At 4 days post-treatment, the surviving worms were analyzed by SEM and TEM. Generally, varying features such as ridges, spines, ciliated hemispherical papillae, and sensory struc-

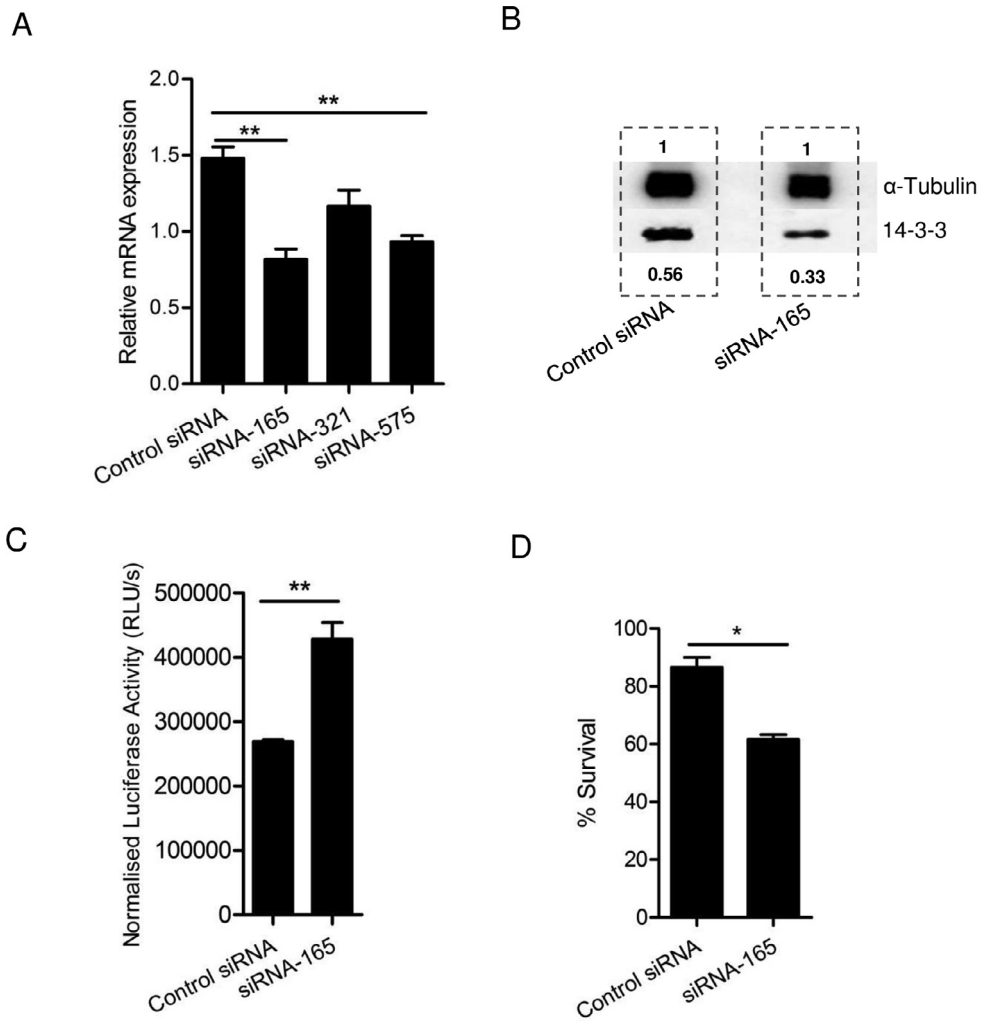

Fig. 3. *Schistosoma japonicum* 14-3-3 (Sj14-3-3) silencing results in increased caspase activity and worm death. (A) Screening of the best small interfering RNA (siRNA) duplex for inhibiting *Sj14-3-3*. Three siRNA duplexes were electroporated into *in vitro* cultured schistosomes and *Sj14-3-3* mRNA levels were determined relative to those of *S. japonicum* nicotinamide adenine dinucleotide dehydrogenase (*SjNADH*) in Sj14-3-3 siRNA- and control siRNA-treated worms at 4 days post-electroporation by quantitative real time PCR (qRT-PCR). Data are representative results and show the mean and S.E. from triplicate experiments. $^{**}P \leq 0.01$. (B) Validation of the siRNA duplex for silencing Sj14-3-3 by western blotting. The values reported under each blot are the mean fold protein expression relative to an α-tubulin control taken as 1 (Image J quantification). (C) Sj14-3-3 silencing resulted in increased caspase 3/7 activity. At 4 days post-treatment, protein lysates of worms were prepared and used to determine caspase 3/7 activity. Data are representative results and show the mean and S.E. from triplicate experiments. $^{**}P \leq 0.01$. RLU, Relative luminometer units. (D) Sj14-3-3 silencing resulted in increased worm death. At 4 days post-treatment, the worms were stained with Hoechst 33258 dye to determine worm death. Data are representative results and show the mean and S.E. from three separate experiments. $^{*}P \leq 0.05$.

tures are found in different regions of the schistosome tegument. We observed that approximately 80% of worms had significant defects in the tegument, such as swollen ridges along with detachment and crumbling of the schistosome tegument, whereas such alterations were not observed in control worms (Fig. 5A), suggesting that Sj14-3-3 and SjUBC silencing compromises the integrity of the tegument. In addition, we examined the ultrastructure of the schistosome tegument in parasites treated with *Sj14-3-3/SjUBC* siRNA by TEM. The results indicated severe defects in tegument architecture, including enlarged vacuoles together with damaged apical and syncytial cytoplasm in the majority of treated worms (Fig. 5B). No such alterations were found in the tegument of worms treated with control siRNA.

4. Discussion

Schistosomes can survive in definitive hosts up to several decades in an adverse hostile environment. The schistosome tegument is considered the most accessible interface for host immune attack. It has been hypothesized that the worm evades the host immune response through surface masking, molecular mimicry, and active modulation of host immune responses, all of which contribute to schistosome survival (Skelly and Alan Wilson, 2006). Studies on the schistosome tegument ultrastructure have revealed its importance in self-maintenance within the mammalian host. Structurally, the tegument consists of a continuous bilayer membrane with an unusual heptalaminate appearance on the surface, which markedly increases the surface area of the schistosome (Hockley, 1973; Gobert et al., 2003). Functional analysis of the tegument has shown that the surface invagination increases the surface area and appears to be the main site of nutrient uptake, which is supported by the presence of multiple transporter proteins for glucose and amino acids (Rogers and Bueding, 1975; Uglem and Read, 1975; Skelly and Shoemaker, 1996). Since blood-dwelling digenean parasites have a heptalaminate tegument, these characterizations are considered an important strategy to adapt to life in the blood stream (McLaren and Hockley, 1977; Wiest et al., 1988).

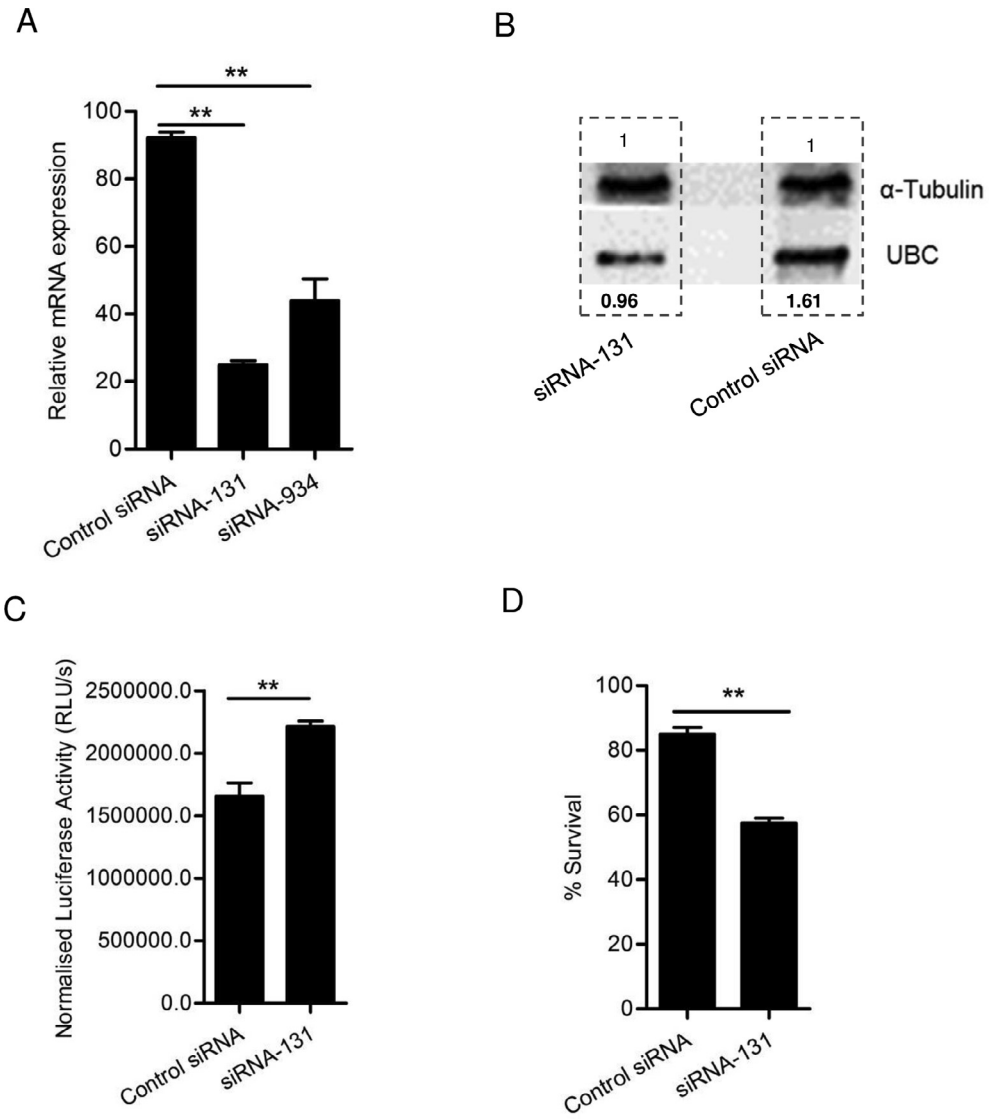

Fig. 4. *Schistosoma japonicum* ubiquitin C (SjUBC) silencing leads to a significant increase in caspase activity and worm death. (A) Screening of the best small interfering RNA (siRNA) duplex for inhibiting *SjUBC*. Two siRNA duplexes were electroporated into *in vitro* cultured schistosomes and *SjUBC* mRNA levels were determined relative to those of *S. japonicum* nicotinamide adenine dinucleotide dehydrogenase (*SjNADH*) in *SjUBC* siRNA- and control siRNA- treated worms at 4 days post-electroporation by quantitative real time PCR (qRT-PCR). Data are representative results and show the mean and S.E. from triplicate experiments. $^{**}P \leq 0.01$. (B) Validation of siRNA-131 duplex for silencing *SjUBC* using western blotting. The values reported under each blot are the mean fold protein expression relative to an α-tubulin control taken as 1 (Image J quantification). (C) SjUBC silencing resulted in increased caspase 3/7 activity. At 4 days post-treatment, protein lysates of worms were prepared and used to determine caspase 3/7 activity. Data are representative results and show the mean and S.E. from triplicate experiments. $^{**}P \leq 0.01$. RLU, Relative luminometer units. (D) SjUBC silencing resulted in increased worm death. At 4 days post-treatment, the viability of worms was determined as described in Section 2. Data are representative results and show the mean and S.E. from three separate experiments. $^{**}P \leq 0.01$.

Previously, we demonstrated that SjIAP in *S. japonicum* governs the integrity of the schistosome tegument by inhibiting cellular apoptosis of the parasite (Liu et al., 2018). To gain insights into the involvement of SjIAP in regulating apoptosis in *S. japonicum*, we screened a Y2HSJ library using SjIAP as the bait plasmid. Bioinformatic analysis indicated the obtained interacting partners included protein domains such as a 14-3-3 homologue, ubiquitin homologue, EF-hand, and others. In addition, 15 interacting partners were shown to belong to no significant domain. These results suggested that SjIAP might have broad effects on the regulation of schistosome development and apoptosis.

Biologically, IAPs can neutralize caspase activity either by directly binding to caspases or by ubiquitinating caspases and targeting them for degradation via the proteasome (Huang et al., 2000; Suzuki et al., 2001). Mammalian IAPs usually contain at least one baculoviral IAP repeat (BIR) domain and have other distinct functional domains such as the really interesting new gene (RING) domain and caspase-recruitment domains (CARDs) (Eckelman et al., 2006). The type II BIR domains contain a surface hydrophobic groove, allowing the interaction with an IAP binding motif (IBM) found in caspase sub-units and IAP antagonists (Berthelet and Dubrez, 2013). In the previous study, we found that *S. japonicum* IAP contains one BIR domain and recombinant SjIAP protein can inhibit caspase activity in adult worm lysates and in transfected mammalian cells (Peng et al., 2010). Structural analysis of SjIAP indicated it is more likely to be type II BIR, which may potentially bind to caspases (Silke and Meier, 2013). However, we did not obtain caspases as interacting partners of SjIAP in the present study, suggesting that future studies will be required to explore the functions of SjIAP BIR domain and its interacting partners.

Among the interacting partners of SjIAP identified by screening the Y2HSJ, we noted that five 14-3-3 homologues might interact

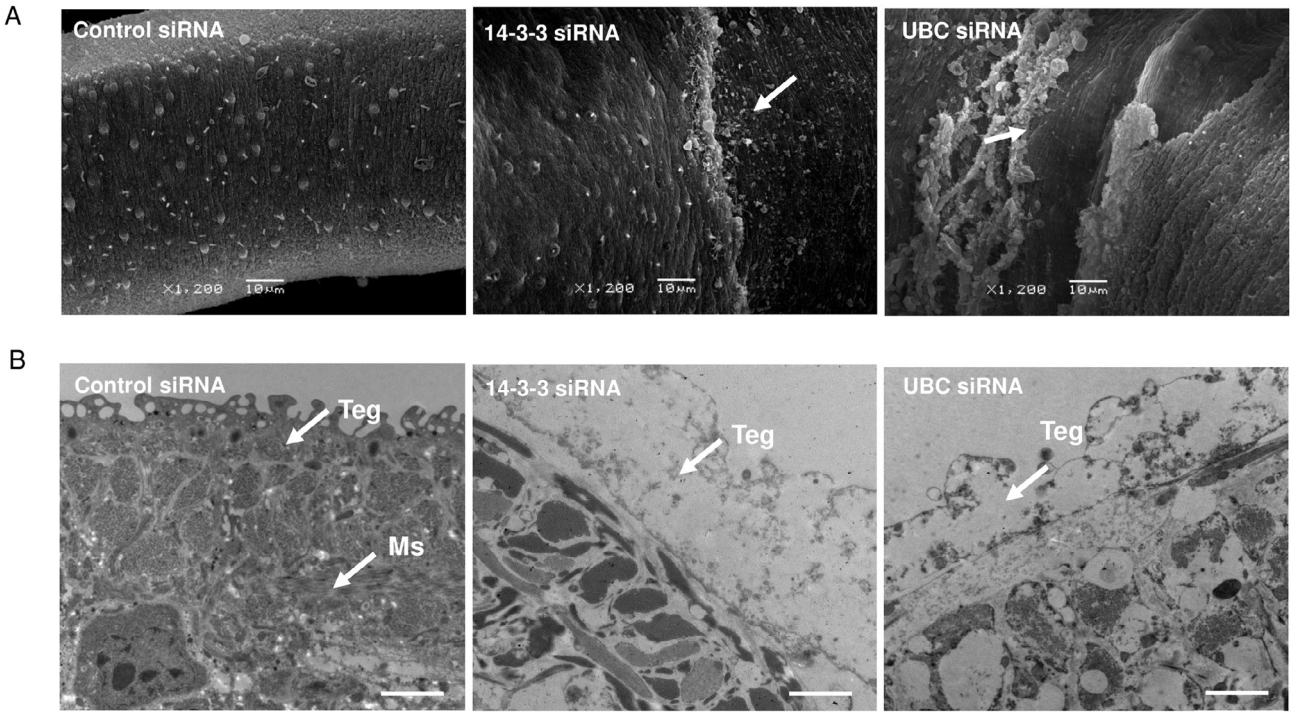

Fig. 5. *Schistosoma japonicum* 14-3-3 (Sj14-3-3) and *S. japonicum* ubiquitin C (SjUBC) inhibition lead to morphological alterations in the tegument of *S. japonicum*. (A) Scanning electron microscopy (SEM) analysis of the tegument of *S. japonicum* following treatment with *Sj14-3-3/SjUBC* small interfering RNA (siRNA). Tegument ridges and sensory structures were observed in the mid-part of the worm body. Arrows indicate tegument destruction. Data are representative results from at least 12 worms investigated in three independent experiments. (B) Transmission electron microscopy (TEM) analysis of the tegument of *S. japonicum* following treatment with *Sj14-3-3/SjUBC* siRNA. Data are representative results from at least 12 worms investigated in three independent experiments. Bars indicate 2 μm. Teg, tegument; Ms, muscle.

with SjIAP. BLAST analysis of these proteins suggested that they can be annotated to two groups. The first group includes FN315545.1 and FN321076.1 that annotated as putative tyrosine 3-monooxygenase. The second group includes FN322774.1, FN322779.1, and FN316174.1 that annotated as tyrosine 3-monooxygenase/tryptophan 5-monooxygenase activation protein, beta polypeptide. The tyrosine 3-monooxygenase belongs to the family of transferases, specifically those transferring a phosphate group to the side chain oxygen atom of serine or threonine residues in proteins. Therefore, 14-3-3 homologues play important roles in the regulation of cell cycle, cell proliferation, and apoptosis. For example, 14-3-3 has been shown to bind to most of its cellular ligands though a phosphorylated motif (Cockrell et al., 2010) and can antagonize apoptosis signal-regulating kinase 1-induced apoptosis (Goldman et al., 2004). Highly controlled signaling regulates pathways involved in cell viability and death, and 14-3-3 is a key protein in these processes as it regulates many of the associated signaling pathway proteins (Pozuelo-Rubio, 2012). The binding of 14-3-3 can alter the enzymatic activity, subcellular localization, protein–protein interactions, phosphorylation status and proteolysis of target proteins (Yaffe, 2002). Different isoforms of 14-3-3 had been identified in schistosomes (McGonigle et al., 2002) and studies on immunolocalization of 14-3-3 indicated that it presents at tegument, subtegument, muscle, parenchyma and in the reproductive system of males and females (Schechtman et al., 2001). In the present study, we noted that Sj14-3-3 is significantly localized to the tegument of *S. japonicum* and that its silencing results in tegument destruction, suggesting that Sj14-3-3 might be involved in maintenance of tegument integrity in *S. japonicum*.

In addition, we also found that UBC is another interacting partner of SjIAP. Previous studies have indicated that the domain for ubiquitin binding is located between the RING and CARD domains of IAP and that ubiquitin binding is an essential mechanism to promote the turnover of auto-ubiquitinated cellular IAPs (cIAPs) (Blankenship et al., 2009). Studies on XIAP ubiquitination have suggested that ubiquitination potentiates or controls the anti-apoptotic effect (Silke and Vucic, 2014). Silencing SjUBC led to increased caspase activity and tegument destruction, suggesting that SjUBC is directly or indirectly involved in the regulation of apoptosis in *S. japonicum*, which has important roles in maintaining tegument integrity in *S. japonicum*. Although we noted Sj14-3-3/SjUBC silencing resulted in tegument destruction, it is necessary to clarify that their silencing may also lead to cell death in other tissues since both of them were shown to ubiquitously express in the bodies of worms. In addition, we noted that SjIAP silencing led to decreased expression of the interacting partner of Sj14-3-3/SjUBC (Fig. 1C), suggesting that the complex of SjIAP and Sj14-3-3/SjUBC may synergistically play an important role in *S. japonicum*.

Overall, we found that silencing Sj14-3-3 or SjUBC results in tegumental surface damage, which was associated with increased worm death. Given that SjIAP localizes to the tegument of *S. japonicum* and that suppressing this protein resulted in the destruction of tegument integrity, our results suggested that the interactions among SjIAP, Sj14-3-3, and SjUBC might represent another strategy of *S. japonicum* to maintain tegument integrity.

Acknowledgements

This study was, in part or in whole, supported by the National Natural Science Foundation of China (31472187 and 31672550) and The Agricultural Science and Technology Innovation Program of the Chinese Academy of Agricultural Sciences.

Appendix A. Supplementary data

Supplementary data to this article can be found online at https://doi.org/10.1016/j.ijpara.2018.11.011.

References

Berthelet, J., Dubrez, L., 2013. Regulation of apoptosis by inhibitors of apoptosis (IAPs). Cells 2, 163–187.

Blankenship, J.W., Varfolomeev, E., Goncharov, T., Fedorova, A.V., Kirkpatrick, D.S., Izrael-Tomasevic, A., Phu, L., Arnott, D., Aghajan, M., Zobel, K., Bazan, J.F., Fairbrother, W.J., Deshayes, K., Vucic, D., 2009. Ubiquitin binding modulates IAP antagonist-stimulated proteasomal degradation of c-IAP1 and c-IAP2(1). Biochem. J. 417, 149–160.

Cheng, G., Luo, R., Hu, C., Lin, J., Bai, Z., Zhang, B., Wang, H., 2013. TiO2-based phosphoproteomic analysis of schistosomes: characterization of phosphorylated proteins in the different stages and sex of *Schistosoma japonicum*. J. Proteome Res. 12, 729–742.

Cheng, G.F., Lin, J.J., Feng, X.G., Fu, Z.Q., Jin, Y.M., Yuan, C.X., Zhou, Y.C., Cai, Y.M., 2005. Proteomic analysis of differentially expressed proteins between the male and female worm of *Schistosoma japonicum* after pairing. Proteomics 5, 511–521.

Clapp, C., Portt, L., Khoury, C., Sheibani, S., Norman, G., Ebner, P., Eid, R., Vali, H., Mandato, C.A., Madeo, F., Greenwood, M.T., 2012. 14-3-3 protects against stress-induced apoptosis. Cell Death Dis. 3, e348.

Cockrell, L.M., Puckett, M.C., Goldman, E.H., Khuri, F.R., Fu, H., 2010. Dual engagement of 14-3-3 proteins controls signal relay from ASK2 to the ASK1 signalosome. Oncogene 29, 822–830.

Colley, D.G., Bustinduy, A.L., Secor, W.E., King, C.H., 2014. Human schistosomiasis. Lancet 383, 2253–2264.

Eckelman, B.P., Salvesen, G.S., Scott, F.L., 2006. Human inhibitor of apoptosis proteins: why XIAP is the black sheep of the family. EMBO Rep. 7, 988–994.

Gobert, G.N., Stenzel, D.J., McManus, D.P., Jones, M.K., 2003. The ultrastructural architecture of the adult *Schistosoma japonicum* tegument. Int. J. Parasitol. 33, 1561–1575.

Goldman, E.H., Chen, L., Fu, H., 2004. Activation of apoptosis signal-regulating kinase 1 by reactive oxygen species through dephosphorylation at serine 967 and 14-3-3 dissociation. J. Biol. Chem. 279, 10442–10449.

Hockley, D., 1973. Ultrastructure of the tegument of *Schistosoma*. Adv. Parasitol. 11, 233–305.

Hotez, P.J., Alvarado, M., Basanez, M.G., Bolliger, I., Bourne, R., Boussinesq, M., Brooker, S.J., Brown, A.S., Buckle, G., Budke, C.M., Carabin, H., Coffeng, L.E., Fevre, E.M., Furst, T., Halasa, Y.A., Jasrasaria, R., Johns, N.E., Keiser, J., King, C.H., Lozano, R., Murdoch, M.E., O'Hanlon, S., Pion, S.D., Pullan, R.L., Ramaiah, K.D., Roberts, T., Shepard, D.S., Smith, J.L., Stolk, W.A., Undurraga, E.A., Utzinger, J., Wang, M., Murray, C.J., Naghavi, M., 2014. The global burden of disease study 2010: interpretation and implications for the neglected tropical diseases. PLoS Negl. Trop. Dis. 8, e2865.

Hu, C., Zhu, L., Luo, R., Dao, J., Zhao, J., Shi, Y., Li, H., Lu, K., Feng, X., Lin, J., Liu, J., Cheng, G., 2014. Evaluation of protective immune response in mice by vaccination the recombinant adenovirus for expressing *Schistosoma japonicum* inhibitor apoptosis protein. Parasitol. Res. 113, 4261–4269.

Hu, S., Yang, X., 2003. Cellular inhibitor of apoptosis 1 and 2 are ubiquitin ligases for the apoptosis inducer Smac/DIABLO. J. Biol. Chem. 278, 10055–10060.

Hu, W., Yan, Q., Shen, D.K., Liu, F., Zhu, Z.D., Song, H.D., Xu, X.R., Wang, Z.J., Rong, Y.P., Zeng, L.C., Wu, J., Zhang, X., Wang, J.J., Xu, X.N., Wang, S.Y., Fu, G., Zhang, X.L., Wang, Z.Q., Brindley, P.J., McManus, D.P., Xue, C.L., Feng, Z., Chen, Z., Han, Z.G., 2003. Evolutionary and biomedical implications of a *Schistosoma japonicum* complementary DNA resource. Nat. Genet. 35, 139–147.

Huang, H., Joazeiro, C.A., Bonfoco, E., Kamada, S., Leverson, J.D., Hunter, T., 2000. The inhibitor of apoptosis, cIAP2, functions as a ubiquitin-protein ligase and promotes *in vitro* monoubiquitination of caspases 3 and 7. J. Biol. Chem. 275, 26661–26664.

Kerr, J.F., Wyllie, A.H., Currie, A.R., 1972. Apoptosis: a basic biological phenomenon with wide-ranging implications in tissue kinetics. Br. J. Cancer 26, 239–257.

Lee, E.F., Clarke, O.B., Evangelista, M., Feng, Z., Speed, T.P., Tchoubrieva, E.B., Strasser, A., Kalinna, B.H., Colman, P.M., Fairlie, W.D., 2011. Discovery and molecular characterization of a Bcl-2-regulated cell death pathway in schistosomes. Proc. Natl. Acad. Sci USA 108, 6999–7003.

Lee, E.F., Young, N.D., Lim, N.T., Gasser, R.B., Fairlie, W.D., 2014. Apoptosis in schistosomes: toward novel targets for the treatment of schistosomiasis. Trends Parasitol. 30, 75–84.

Lewis, F.A., Stirewalt, M.A., Souza, C.P., Gazzinelli, G., 1986. Large-scale laboratory maintenance of *Schistosoma mansoni*, with observations on three schistosome/snail host combinations. J. Parasitol. 72, 813–829.

Liu, J., Giri, B., Chen, Y., Luo, R., Xia, T., Grevelding, C., Cheng, G., 2018. *Schistosoma japonicum* IAP and Teg20 safeguard tegumental integrity by inhibiting cellular apoptosis. PLoS Negl. Trop. Dis. 12, e0006654.

Livak, K.J., Schmittgen, T.D., 2001. Analysis of relative gene expression data using real-time quantitative PCR and the 2(-Delta Delta C(T)) Method. Methods 25, 402–408.

McGonigle, S., Loschiavo, M., Pearce, E.J., 2002. 14-3-3 proteins in *Schistosoma mansoni*; identification of a second epsilon isoform. Int. J. Parasitol. 32, 685–693.

McLaren, D.J., Hockley, D.J., 1977. Blood flukes have a double outer membrane. Nature 269, 147–149.

Peng, J., Yang, Y., Feng, X., Cheng, G., Lin, J., 2010. Molecular characterizations of an inhibitor of apoptosis from *Schistosoma japonicum*. Parasitol. Res. 106, 967–976.

Peng, J., Gobert, G.N., Hong, Y., Jiang, W., Han, H., McManus, D.P., Wang, X., Liu, J., Fu, Z., Shi, Y., Lin, J., 2011. Apoptosis governs the elimination of *Schistosoma japonicum* from the non-permissive host *Microtus fortis*. PLoS One 6, e21109.

Pozuelo-Rubio, M., 2012. 14-3-3 proteins are regulators of autophagy. Cells 1, 754–773.

Rogers, S.H., Bueding, E., 1975. Anatomical localization of glucose uptake by *Schistosoma mansoni* adults. Int. J. Parasitol. 5, 369–371.

Schechtman, D., Winnen, R., Tarrab-Hazdai, R., Ram, D., Shinder, V., Grevelding, C.G., Kunz, W., Arnon, R., 2001. Expression and immunolocalization of the 14-3-3 protein of *Schistosoma mansoni*. Parasitology 123, 573–582.

Scott, F.L., Denault, J.B., Riedl, S.J., Shin, H., Renatus, M., Salvesen, G.S., 2005. XIAP inhibits caspase-3 and -7 using two binding sites: evolutionarily conserved mechanism of IAPs. EMBO J. 24, 645–655.

Silke, J., Meier, P., 2013. Inhibitor of apoptosis (IAP) proteins-modulators of cell death and inflammation. Cold Spring Harb. Perspect. Biol. 5, a008730.

Silke, J., Vucic, D., 2014. IAP family of cell death and signaling regulators. Methods Enzymol. 545, 35–65.

Skelly, P.J., Shoemaker, C.B., 1996. Rapid appearance and asymmetric distribution of glucose transporter SGTP4 at the apical surface of intramammalian-stage *Schistosoma mansoni*. Proc. Natl. Acad. Sci. USA 93, 3642–3646.

Skelly, P.J., Alan Wilson, R., 2006. Making sense of the schistosome surface. Adv. Parasitol. 63, 185–284.

Srinivasula, S.M., Ashwell, J.D., 2008. IAPs: what's in a name? Mol. Cell 30, 123–135.

Suzuki, Y., Nakabayashi, Y., Takahashi, R., 2001. Ubiquitin-protein ligase activity of X-linked inhibitor of apoptosis protein promotes proteasomal degradation of caspase-3 and enhances its anti-apoptotic effect in Fas-induced cell death. Proc. Natl. Acad. Sci. USA 98, 8662–8667.

Thetiot-Laurent, S.A., Boissier, J., Robert, A., Meunier, B., 2013. Schistosomiasis chemotherapy. Angew. Chem. Int. Ed. Engl. 52, 7936–7956.

Uglem, G.L., Read, C.P., 1975. Sugar transport and metabolism in *Schistosoma mansoni*. J. Parasitol. 61, 390–397.

Vale, N., Gouveia, M.J., Rinaldi, G., Brindley, P.J., Gartner, F., Correia da Costa, J.M., 2017. Praziquantel for Schistosomiasis: single-drug metabolism revisited, mode of action, and resistance. Antimicrob. Agents Chemother. 61, e02582–16.

Wiest, P.M., Tartakoff, A.M., Aikawa, M., Mahmoud, A.A., 1988. Inhibition of surface membrane maturation in schistosomula of *Schistosoma mansoni*. Proc. Natl. Acad. Sci. USA 85, 3825–3829.

Williams, G.T., 1994. Programmed cell death: a fundamental protective response to pathogens. Trends Microbiol. 2, 463–464.

Yaffe, M.B., 2002. How do 14-3-3 proteins work?– Gatekeeper phosphorylation and the molecular anvil hypothesis. FEBS Lett. 513, 53–57.